THE JOURNAL OF BIOLOGICAL CHEMISTRY VOL. 286, NO. 18, pp. 15943–15954, May 6, 2011

Sts-2 Is a Phosphatase That Negatively Regulates Zeta-associated Protein (ZAP)-70 and T Cell Receptor Signaling Pathways*[S]

Received for publication, August 22, 2010, and in revised form, March 6, 2011 Published, JBC Papers in Press, March 10, 2011, DOI 10.1074/jbc.M110.177634

Boris San Luis[‡], Ben Sondgeroth[§], Nicolas Nassar[§1], and Nick Carpino[‡2]

From the Departments of [‡]Molecular Genetics and Microbiology and [§]Physiology and Biophysics, Stony Brook University, Stony Brook, New York 11794

T cell activity is controlled in large part by the T cell receptor (TCR). The TCR detects the presence of foreign pathogens and activates the T cell-mediated immune reaction. Numerous intracellular signaling pathways downstream of the TCR are involved in the process of T cell activation. Negative regulation of these pathways helps prevent excessive and deleterious T cell responses. Two homologous proteins, Sts-1 and Sts-2, have been shown to function as critical negative regulators of TCR signaling. The phosphoglycerate mutase-like domain of Sts-1 (Sts-1_{PGM}) has a potent phosphatase activity that contributes to the suppression of TCR signaling. The function of Sts-2_{PGM} as a phosphatase has been less clear, principally because its intrinsic enzyme activity has been difficult to detect. Here, we demonstrate that Sts-2 regulates the level of tyrosine phosphorylation on targets within T cells, among them the critical T cell tyrosine kinase Zap-70. Utilizing new phosphorylated substrates, we demonstrate that Sts-2_{PGM} has clear, albeit weak, phosphatase activity. We further pinpoint Sts-2 residues Glu-481, Ser-552, and Ser-582 as specificity determinants, in that an Sts-2_{PGM} triple mutant in which these three amino acids are altered to their counterparts in Sts-1_{PGM} has substantially increased activity. Our results suggest that the phosphatase activities of both suppressor of TCR signaling homologues cooperate in a similar but independent fashion to help set the threshold for TCR-induced T cell activation.

Within the immune system, T cells play an instrumental role in eliminating foreign pathogens. They do so either directly, by killing cells that harbor deleterious microbes, or indirectly, by secreting a variety of different cytokines that help orchestrate the responses of many other cell types (1, 2). T cells become activated following stimulation of a surface receptor known as the T cell receptor (TCR).[3] Engagement of the TCR activates an array of intracellular signaling cascades (3). As part of the process to ensure T cells are only activated within the appropriate immune context, these signaling pathways are tightly regulated by a variety of overlapping mechanisms (4). Two proteins that belong to the suppressor of TCR signaling family, Sts-1 and Sts-2, have been identified as negative regulators of TCR signaling (5). Within T cells, the Sts proteins appear to regulate elements of intracellular signaling cascades that are proximal to the TCR, including the important T cell kinase Zap-70 and a number of unknown proteins that are rapidly modified by tyrosine phosphorylation and ubiquitination following TCR stimulation (6). The important role of Sts-1 and Sts-2 in controlling cellular responses is underscored by the hyper-reactivity of T cells that lack both proteins and the susceptibility to auto-immunity of mice in which both genes have been genetically ablated (7).

Sts-1 and Sts-2 are characterized by a unique tripartite structure composed of an N-terminal ubiquitin association (UBA) domain that can bind mono- and polyubiquitin (8), a central Src homology 3 (SH3) domain that interacts with proline-rich segments of other polypeptides, and a C-terminal PGM domain that has limited sequence homology to members of the phosphoglycerate mutase (PGM)/acid phosphatase (AcP) superfamily of enzymes. PGM/AcP enzymes possess phosphatase or phosphotransferase catalytic activity and are characterized by a common tertiary structure (9). They are also referred to as 2H-phosphatases because their catalytic mechanism relies on two signature histidines that are conserved in all members of the superfamily (10). Superfamily members include such diverse enzymes as phosphoglycerate mutase, fructose-2,6-bisphosphatase, prostatic acid phosphatase, and bacterial phosphatase SixA. Despite limited primary amino acid sequence homology to PGM family members, both Sts-1_{PGM} and Sts-2_{PGM} possess the critical catalytic residues and adopt the overall fold that characterizes all PGM enzymes (11, 12).

T cells that lack the Sts proteins (*Sts-1/2*$^{-/-}$) display hyperphosphorylation of the protein-tyrosine kinase Zap-70 following TCR stimulation (7). In addition, hyper-phosphorylation of a number of unknown ubiquitinated proteins that are gener-

* This work was supported, in whole or in part, by National Institutes of Health Grants R21AI075176 and R01AI080892 from NIAID and CA-115611 (to N. N.). This work was also supported by Stony Brook University, Grant LI07 from the Arthritis Foundation (to N. C.), and Department of Defense Grant NF060060 (to N. N.).

[S] The on-line version of this article (available at http://www.jbc.org) contains supplemental Figs. S1 and S2.

[1] Present address: Division of Experimental Hematology and Cancer Biology, Children's Hospital Medical Center, MLC 7013, 3333 Burnet Ave., Cincinnati, OH 45229.

[2] To whom correspondence should be addressed: Rm. 160 Life Science Bldg., Stony Brook University, Stony Brook, NY 11794. Tel.: 631-632-4610; Fax: 631-632-9797; E-mail: ncarpino@notes.cc.sunysb.edu.

[3] The abbreviations used are: TCR, T cell receptor; PGM, phosphoglycerate mutase; Sts, suppressor of TCR signaling; UBA, ubiquitin association; SH3, Src homology 3; AcP, acid phosphatase; pNPP, *para*-nitrophenyl phosphate; OMFP, 3-*O*-methylfluorescein phosphate; FDP, fluorescein diphosphate; PLC, phospholipase C.

ated following TCR engagement is evident in T cells lacking Sts-1 and Sts-2 (6). These observations led to the hypothesis that Sts-1 and Sts-2 were intracellular phosphatases and that their substrates were tyrosine-phosphorylated components of TCR signaling pathways. Consistent with this model, the PGM domain of Sts-1 was demonstrated to have *in vitro* tyrosine phosphatase activity (11). In particular, it was shown to have the capacity to efficiently hydrolyze the nonspecific phosphatase substrate *para*-nitrophenyl-phosphate (pNPP), a Tyr(P) analogue, as well as tyrosine-phosphorylated peptides and proteins (13). In addition, Sts-1 was found to readily target numerous substrates within cells, including the tyrosine kinases Zap-70, Syk, and the EGF receptor (11, 14, 15). In contrast, Sts-2_{PGM} *in vitro* phosphatase activity toward pNPP was found to be 5 orders of magnitude weaker than the activity of Sts-1_{PGM}, despite the presence of all conserved catalytic residues. Additionally, Sts-2_{PGM} does not dephosphorylate tyrosine-phosphorylated peptides and proteins *in vitro* (12) nor does Sts-2 target tyrosine-phosphorylated substrates similar to Sts-1 when it is overexpressed in cells (14, 16). The catalytic inefficiency of Sts-2_{PGM} has led to speculation that Sts-2 either has a very narrow substrate range or, alternatively, that it does not function as an intracellular phosphatase within T cells (5, 11, 17).

To more precisely define the role of Sts-2 in regulating TCR signaling pathways, we undertook an investigation into its specific functional and biochemical properties. Our results support a model in which Sts-2, along with Sts-1, is involved in the dephosphorylation and down-regulation of key components within the TCR signaling pathways.

EXPERIMENTAL PROCEDURES

Chemicals, Antibodies, and Reagents—All chemicals and antibodies except as noted below were obtained from Sigma. Ten millimolar stock solutions of pNPP, 3-*O*-methylfluorescein phosphate (OMFP), and fluorescein diphosphate (FDP, Anaspec, Inc.) were prepared either in water (pNPP) or DMSO and stored at −20 °C. Recombinant human IL-2 was purchased from PeproTech, Inc., and the following reagents for stimulating T cells were obtained from BD Biosciences, anti-CD3 (145-2C11), biotinylated anti-CD3 (500A2), biotinylated anti-CD4 (RM4-5), biotinylated anti-CD-8 (53-6.7), and streptavidin. Anti-Tyr(P) mAb 4G10 was from Millipore; anti-ubiquitin mAb and anti-Zap-70 Tyr(P)-292 antibodies were from Invitrogen; anti-Zap-70 mAb (1E7.2) and anti-PLCγ1 (1249) antibodies were from Santa Cruz Biotechnology, and the following antibodies were obtained from Cell Signaling Technology: anti-Zap-70 Tyr(P)-493, anti-Zap-70 Tyr(P)-319, anti-PLCγ1 Tyr(P)-783, anti-p42/p44 MAPK mAb (3A7), and anti-phospho-p42/p44 MAPK. Secondary antibodies were Alexa Fluor® 680-conjugated goat anti-mouse from Invitrogen and IRDye800-conjugated goat anti-rabbit secondary antibodies from LI-COR. Rabbit polyclonal antibodies to Sts-2 and Sts-1 were described previously (7, 18). Recombinant phosphatase 1B (PTP1B) was from Biomol International, Inc.

Mice—The Sts mutations were back-crossed as heterozygote mutations through 10 generations of wild-type Bl/6 mice, following which *Sts-1*$^{-/-}$, *Sts-2*$^{-/-}$, and *Sts-1/2*$^{-/-}$ mice were obtained by the appropriate matings. Mice were housed and bred under specific pathogen-free conditions according to institutional guidelines. Animal work was conducted under guidelines established and approved by the Stony Brook Institutional Animal Care and Use Committee.

Cell Culture, T Cell Stimulations, and Transient Transfections—Primary murine T cells were obtained from spleens dissected from wild-type, *Sts-1*$^{-/-}$, *Sts-2*$^{-/-}$, and *Sts-1/2*$^{-/-}$ mice. To generate activated T cells, spleens were crushed in PBS containing 2% FBS; red blood cells were lysed by addition of ACK lysis buffer, pH 7.2, containing 150 mM NH_4Cl, 1 mM $KHCO_3$, and 0.1 mM EDTA, and debris was removed by straining through a 70-μm filter (BD Biosciences). Total splenocyte cultures were established, and T cells were activated and expanded for 2 days in T cell medium (RPMI 1640 media containing 10% FCS, 10 mM HEPES, pH 7.0, 2 mM glutamine, 1 mM sodium pyruvate, 50 μM β-mercaptoethanol, 0.1 mM nonessential amino acids, and the appropriate concentration of penicillin/streptomycin, all from Invitrogen) supplemented with 0.5 μg/ml anti-TCR antibody 145-2C11 and 2 units/ml recombinant human IL-2. The T cells cultures were further expanded for 2 more days in fresh T cell media containing IL-2, collected by centrifugation, and utilized for biochemical analyses. Activated T cells that had been expanded in IL-2 for 4 days (2×10^7/point) were labeled on ice for 25 min with 20 μg/ml biotinylated anti-CD3, anti-CD4, and anti-CD8. They were then washed with 2% FBS in PBS, incubated for 20 on ice with 10 μg/ml streptavidin, placed in a 37 °C waterbath for 2 min, and immediately lysed in cold lysis buffer (see below). Illustrated results are representative of multiple ($\geq$3) assays. HEK293 cells were cultured in DMEM (Invitrogen), supplemented with 10% FCS and penicillin/streptomycin. DNAs were transiently transfected into 293 cells by calcium phosphate-mediated transfection.

Cell Lysis, Immunoprecipitations, and Immunoblots—Cells were lysed in ice-cold lysis buffer containing 50 mM Tris, pH 7.6, 150 mM NaCl, 5 mM EDTA, 1 mM EGTA, 1 mM Na_3VO_4, 1% Nonidet P-40 substitute Igepal™ CA-630 (United States Biochemical Corp.), 100 μM PMSF, and Complete™ protease inhibitors (Roche Applied Science). Cell lysates were clarified by centrifugation and then either mixed with an equal volume of Laemmli sample buffer or processed for immunoprecipitation analysis. For immunoprecipitations, lysates were rotated at 4 °C with specific antibody and 20 μl of protein A-Sepharose 50% slurry (Sigma) for 1–2 h. Beads were washed three times with cold wash buffer (20 mM Tris, pH 7.6, 150 mM NaCl, 1 mM EDTA, 0.1% Nonidet P-40 substitute, 100 μM PMSF, and 1 mM Na_3VO_4), and bound proteins were eluted with Laemmli sample buffer and separated by SDS-PAGE. Proteins were transferred to either nitrocellulose (Whatman) or PVDF (Millipore) using a semidry transfer apparatus (Bio-Rad), blocked with 3% BSA in Tris-buffered saline (TBS, pH 8.0), incubated at 23 °C for 1 h or 4 °C overnight with specific antibody, washed with TBS, incubated for 1 h with the appropriate secondary antibody, and developed with the ODYSSEY Infrared Imaging System (LI-COR).

Expression of Recombinant Sts$_{PGM}$ Domains—Bacterial expression constructs of Sts-2_{PGM} and Sts-1_{PGM} were generated by excising the Sts PGM coding sequences from the pProEX-

Htb vector (12, 19) with BamHI and SalI and inserting them into the pMAL-c4X vector (New England Biolabs). Maltose-binding protein-Sts_{PGM} fusion proteins were expressed in *Escherichia coli* K12 cells and purified by affinity chromatography using amylose resin columns following the manufacturer's suggested protocol (New England Biolabs). Briefly, a 1-liter culture of cells was grown to A_{600} ~0.5, induced with 0.3 mM isopropyl 1-thio-β-D-galactopyranoside for 3 h at 37 °C, harvested by centrifugation, resuspended 1:5 in column buffer (20 mM Tris-HCl, pH 7.4, 200 mM NaCl, 1 mM EDTA and 10 mM β-mercaptoethanol), and frozen overnight at −20 °C, prior to lysis by sonication. The crude extract was loaded into an amylose resin column (15-ml bed volume) at a flow rate of 1 ml/min, and the fusion protein was eluted with 10 mM maltose in column buffer, collecting 3-ml fractions. Fractions containing the fusion proteins were identified by SDS-PAGE/Coomassie staining, pooled, dialyzed overnight in a 20 mM Tris-HCl buffer, pH 8.0, containing 25 mM NaCl. For further purification, the dialyzed sample was loaded into a DEAE-Sepharose ion-exchange column (6 ml bed volume) and step-eluted starting from 25 to 300 mM NaCl in 20 mM Tris-HCl buffer, pH 8.0. MBP-Sts_{PGM}-containing fractions were pooled and concentrated using an Amicon Ultra-15 centrifugal filter device with a 5-kDa cutoff (Millipore).

Mammalian Sts_{PGM} Expression Constructs—To generate mammalian expression constructs, the wild-type PGM domains of the Sts-1 and Sts-2 were PCR-amplified from Sts cDNAs using forward primers that contained Kozak sequences (Sts-1_{PGM}, 5′-CTCAGTTCTAGAGAATTCGCCGCCACCATGGGACCCCAGAAGCGATCG-3′, and Sts-2_{PGM}, 5′-GCTTCTGATATCGCCGCCACCATGGCTACCATCTCGAGGAGAGGC-3′) and reverse primers that contained FLAG tag coding sequences (Sts-1_{PGM}, 5′-TGGCACGGTACCGCTAGCAGGCCTTTACTTGTCGTCGTCGTCCTTGTAGTCGCCGCCGCCTTCTTGCAGGAGGGTCTC-3′, and Sts-2_{PGM}, 5′-TGGGACGGTACCGCTAGCAGGCCTTCACTTGTCGTCGTCGTCGTCCTTGTAGTCGCCGCCGCCGTTGCTTGAGATCCAGTT-3′). DNAs were subcloned into a modified pmaxGFP vector (Amaxa Biosystems) that contained an IRES-GFP coding sequence substituted for the GFP coding sequence. Sts-2_{PGM} mutants H366C, R448A, and H551A were generated by PCR-based mutagenesis (H366C, forward primer 5′-CTCTCCGGATCCGCTACCATCTCGAGGAGAGGCATTCTGGTCATACGTTGTGGCGAGAGAGTGGAC-3′ and reverse primer T7; R448A, forward primer 5′-TTCGCGTCTCCAGCCCTGGCCTGCGTGCAGACAGCCAAG-3′ and reverse primer 5′-CTTGCCTGTCTGCACGCA-GGCCAGGGCTGGAGACGCGAA-3′; and H551A, forward primer 5′-ATTACACTCATCGTGAGCGCCAGCTCAGCGCTCGACTCC-3′ and reverse primer 5′-GGAGTCGAGCGCTGAGCTGGCGCTCACGATGAGTGTAAT-3′). All constructs generated by PCR were confirmed error-free by sequence analysis.

Enzymes Assays—Continuous phosphatase assays (100 μl of reaction volume) were conducted in 96-well flat-bottom plates (BD Biosciences) using a SpectraMax 190 Microplate reader (Molecular Devices) in buffer containing 25 mM HEPES, pH 7.2, or 50 mM MES, pH 6.0, 50 mM NaCl, 5 mM DTT, 2.5 mM EDTA, and 0.1 mg/ml BSA. Phosphate hydrolysis of pNPP (ϵ, 17,800 M^{-1} cm^{-1}) was monitored by measuring absorbance at 405 nm. Dephosphorylation of OMFP (ϵ, 27,000 M^{-1} cm^{-1}) and FDP (ϵ, 34,000 M^{-1} cm^{-1}) was monitored by measuring absorbance at 477 and 450 nm, respectively. Assays were conducted at 37 °C, and no-enzyme controls were included as blanks. To determine kinetic parameters, substrate saturation curves were prepared from initial velocities using 150 nM Sts-2_{PGM} and 15 nM Sts-1_{PGM} with increasing substrate concentrations. The Michaelis-Menten constant K_m and turnover rate k_{cat} were determined using a dynamic curve fitting function in SigmaPlot 11 (Systat Software, Inc.) to a one-site saturation, ligand binding equation, $y = B_{max}x/(K_D + x)$. End point assays were conducted to measure the phosphatase activity of FLAG-tagged Sts_{PGM} transiently expressed in HEK293 cells. Briefly, FLAG-M2 immunoprecipitates immobilized on protein A-Sepharose beads were washed three times with assay buffer then incubated in 100 μl of assay buffer-containing substrate. The beads were incubated at 37 °C, and the reactions were allowed to proceed for the time specified in the figure legends. Reactions were stopped by incubating on ice for 5 min and collecting the supernatants to measure absorbance of hydrolysis products. Laemmli sample buffer was added to the beads to determine levels of FLAG-tagged Sts_{PGM} by SDS-PAGE and immunoblotting. Assays were performed in triplicate, and immunoprecipitations from empty vector transfections were used as blanks.

Intracellular Cytokine Analysis—Activated T cells (2×10^5) from wild-type and mutant mice were stimulated in triplicate with 0.1 μg/ml plate-bound anti-CD3 (145-2C11, BD Biosciences). Following 6 h of stimulation, cells were treated for 2 h with brefeldin A and processed for intracellular IFNγ staining using the Cytofix/Cytoperm Fixation/Permeabilization kit (BD Biosciences) according to the manufacturer's instructions. Analysis was conducted on a FACSCalibur.

RESULTS

Regulation of Zap-70 Tyrosine Phosphorylation by Sts-2—To assess the individual roles of Sts-1 and Sts-2 in regulating Zap-70 activation, we utilized T cells derived from wild-type, *Sts-1*$^{-/-}$, *Sts-2*$^{-/-}$, and *Sts-1/2*$^{-/-}$ mice (supplemental Fig. S1). Cells were stimulated and lysed, and total cytoplasmic proteins were separated by gel electrophoresis. The levels of phosphorylation of the three Zap-70 tyrosines, Tyr-493, Tyr-319, and Tyr-292, were then determined using phospho-specific antibodies. Each of these tyrosines has been shown to play unique functional roles; Tyr-493 is located in the activation loop of the Zap-70 kinase domain, and its phosphorylation plays a positive regulatory role; Tyr-319 is also thought to play a positive signaling role through its ability to recruit PLCγ; and Tyr-292 appears to play a negative regulatory role, although the mechanism is not completely understood (20, 21). The data in Fig. 1 (*A*, *C*, and *E*) demonstrates differences in the relative levels of Zap-70 site-specific tyrosine phosphorylation in T cells derived from wild-type and mutant mice. Although there was no statistically significant difference between phosphorylation levels observed within *Sts-2*$^{-/-}$ and wild-type T cells, there was a clear difference between *Sts-1*$^{-/-}$ and *Sts-1/2*$^{-/-}$ cells. Thus, although the absence of Sts-2 alone had no readily apparent effect on Zap-70, maximal hyper-phosphorylation at distinct

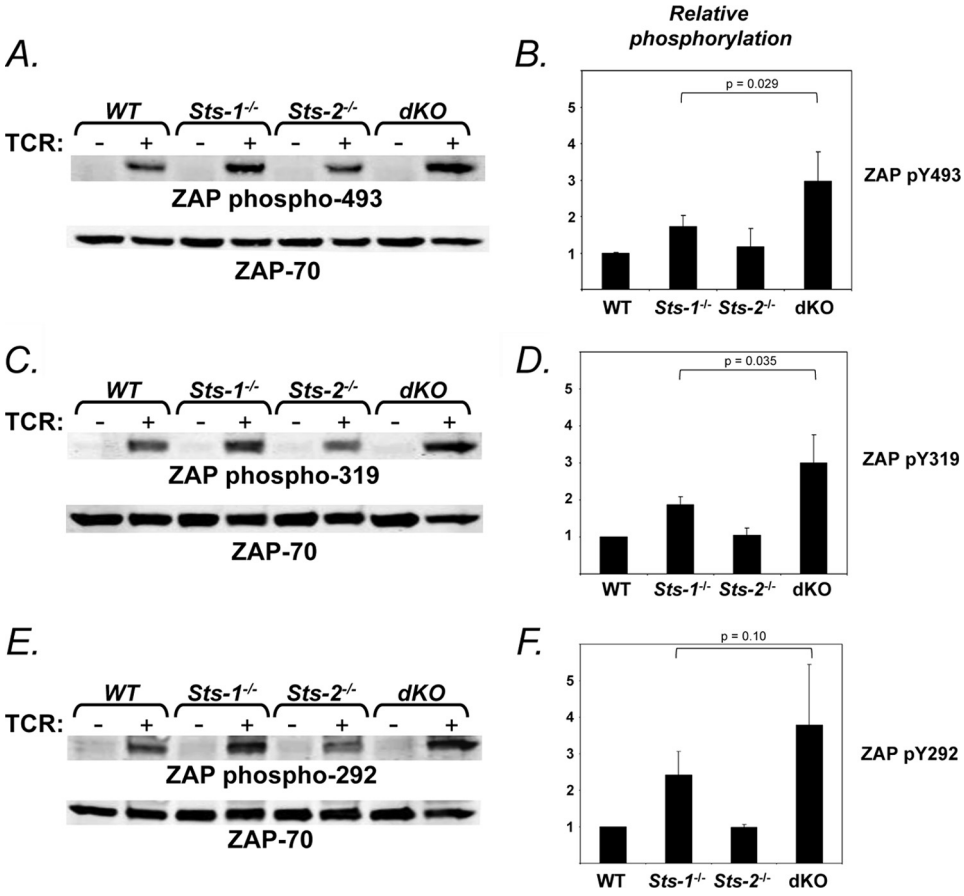

FIGURE 1. **Role for both Sts-2 and Sts-1 in regulating levels of tyrosine-phosphorylated Zap-70.** Wild-type, *Sts-1*$^{-/-}$, *Sts-2*$^{-/-}$, and *Sts-1/2*$^{-/-}$ splenic T cells that had been cultured and expanded for 4 days in the presence of IL-2 were either left untreated or treated with stimulatory antibodies to the surface receptors CD3, CD4, and CD8. Following stimulation, lysates were prepared, and proteins were separated by SDS-PAGE and transferred to nitrocellulose. *A, C,* and *E,* Western analysis with phospho-specific antibodies to Zap-70 Tyr-493, Tyr-319, and Tyr-292 was utilized to determine the levels of site-specific Zap-70 phosphorylation following T cell stimulation. Blots were then reprobed with Zap-70-specific antibodies to assess the levels of native Zap-70 protein. Representative blots are illustrated. *B, D,* and *F,* relative level of site-specific phosphorylation at Zap-70 Tyr-493, Tyr-319, and Tyr-292 was determined by quantifying the fluorescent intensities of the protein bands using a LI-COR Odyssey Imaging System. Each measurement was then normalized to the level of total Zap-70 protein and expressed as a value relative to the normalized level of site-specific phosphorylation observed in wild-type cells. The illustrated data represent the average of three separate experiments. *dKO*, double knock-out.

Zap-70 tyrosine phosphorylation sites required the absence of both Sts-2 and Sts-1. This suggests that each Sts protein functions as a separate and distinct negative regulator of Zap-70 signaling, with Sts-2 having a weaker effect than Sts-1. That they do not function equivalently is suggested by the fact that the absence of Sts-1 consistently produced higher levels of relative phosphorylation than the absence of Sts-2 (see quantification, Fig. 1, *B, D,* and *F*). Whether this is due to differences in the intrinsic phosphatase catalytic properties of the different Sts PGM domains or the involvement of Sts domains or other factors is currently unclear (see below).

Regulation of Tyrosine-phosphorylated, Ubiquitinated Proteins by Sts-2—In addition to targeting Zap-70 for dephosphorylation and down-regulation, the Sts proteins have been shown to be instrumental in down-modulating T cell proteins that are dually modified by both tyrosine phosphorylation and ubiquitination following engagement of the TCR (6). In particular, *Sts-1/2*$^{-/-}$ T cells display strikingly elevated levels of dually modified proteins following TCR stimulation. The extent to which each Sts protein individually contributes to the down-regulation of tyrosine-phosphorylated, ubiquitinated polypeptides is unclear. To assess the individual contributions of Sts-1 and Sts-2, we compared levels of ubiquitinated proteins in phosphotyrosine immunocomplexes isolated from stimulated *Sts-1*$^{-/-}$ or *Sts-2*$^{-/-}$ T cells to those obtained from *Sts-1/2*$^{-/-}$ T cells. Compared with the latter, T cells isolated from Sts singly deficient mice accumulated significantly reduced levels of proteins that were dually modified by tyrosine phosphorylation and ubiquitination (Fig. 2). As in the case of Zap-70 phosphorylation levels, the absence of Sts-1 produced a stronger effect than the absence of Sts-2. In particular, the level of dually modified proteins observed in *Sts-2*$^{-/-}$ T cells was considerably less than the level observed in *Sts-1*$^{-/-}$ T cells.

Regulation of Downstream Signaling Pathways by Sts-2—The absence of both Sts proteins in T cells leads to hyper-activation of downstream signaling pathways, a result that likely stems from deregulation of TCR proximal kinases such as Zap-70 (7). Although the individual contributions of each Sts protein have not been evaluated, the results outlined above suggest that both Sts proteins play distinct roles in the regulation of downstream signaling pathways. To determine the contribution of each Sts protein to the activation of downstream signaling cascades, we

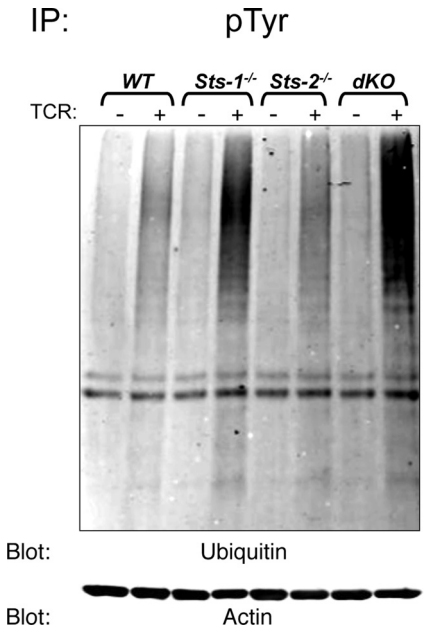

FIGURE 2. **Independent roles for Sts-2 and Sts-1 in regulating levels of tyrosine-phosphorylated and ubiquitinated proteins in stimulated T cells.** Wild-type, *Sts-1*$^{-/-}$, *Sts-2*$^{-/-}$, and *Sts-1/2*$^{-/-}$ splenic T cells that had been cultured and expanded for 4 days in the presence of IL-2 were stimulated as described in Fig. 1. Tyrosine-phosphorylated (*pTyr*) proteins were isolated by immunoprecipitation (*IP*), and levels of proteins that were dually modified by tyrosine phosphorylation and ubiquitination were assessed by anti-ubiquitin Western analysis. An anti-actin immunoblot serves as a loading control. Quantitation of fluorescent intensities in three separate experiments demonstrated the difference between levels of dually modified proteins in *Sts-1*$^{-/-}$ *versus Sts-1/2*$^{-/-}$ was statistically significant: in paired Student *t* test, $p = 0.012$. *dKO*, double knock-out.

compared both the activation of calcium signaling pathways and the activation of MAPK in T cells derived from wild-type, *Sts-1*$^{-/-}$, *Sts-2*$^{-/-}$, and *Sts-1/2*$^{-/-}$ mice. The enzyme PLCγ1 is an essential mediator of intracellular calcium fluxes because it generates key secondary messengers such as inositol 1,4,5-trisphosphate (22). PLCγ1 is activated, in part, by tyrosine phosphorylation that is thought to be induced by TCR proximal kinases (23). To evaluate the individual contributions of Sts-1 and Sts-2 to the state of PLCγ1 activation, lysates derived from unstimulated and stimulated T cells were prepared, and the levels of activated PLCγ1 were assessed by Western analysis utilizing a phosphorylation-specific antibody directed against PLCγ1 Tyr-783. The results mirrored those obtained in the analysis of Zap-70 phosphorylation. Specifically, *Sts-1*$^{-/-}$ and *Sts-2*$^{-/-}$ T cells each displayed levels of phosphorylation on PLCγ1 Tyr-783 that were elevated over those observed in wild-type cells but less than the level observed in *Sts-1/2*$^{-/-}$ T cells. In addition, loss of Sts-2 alone had less of an effect on PLCγ1 activation than loss of Sts-1. Downstream of PLCγ1, levels of MAPK activation in stimulated *Sts-1*$^{-/-}$ and *Sts-2*$^{-/-}$ T cells were found to be greater than in wild-type cells but less than that observed in *Sts-1/2*$^{-/-}$ cells (Fig. 3*B*). These data suggest that Sts-1 and Sts-2 contribute distinct, nonredundant negative regulatory functions within T cells to modulate the levels of activation of downstream calcium signaling pathways and MAPK signaling.

Regulation of IFNγ Production by the Sts Proteins—Activation of intracellular signaling cascades downstream of the TCR leads to the expression of a variety of different cytokine genes. The specific combinations of cytokines and their levels of expression are determined by the developmental state of the T

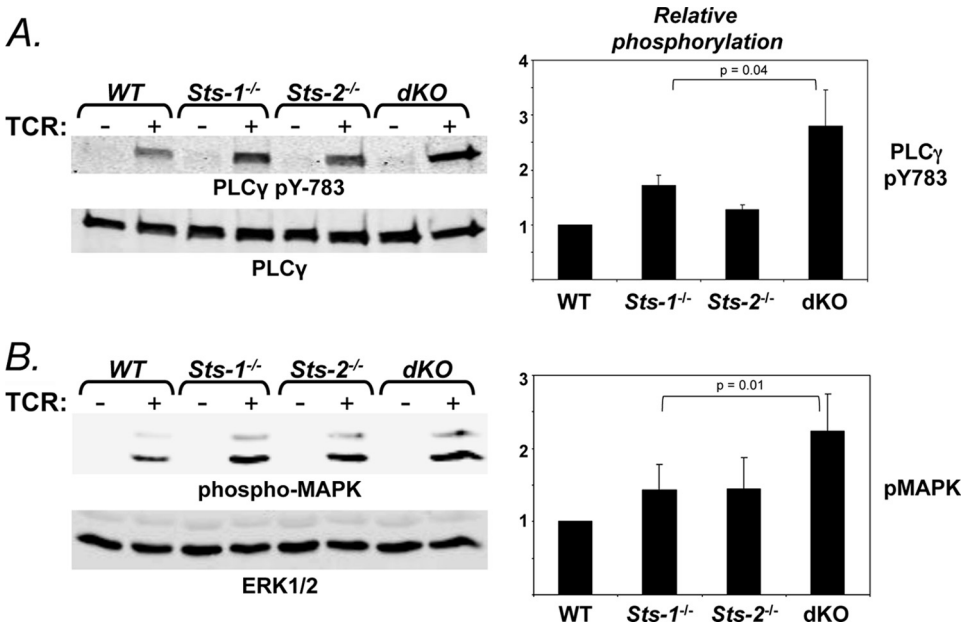

FIGURE 3. **Role for both Sts-2 and Sts-1 in regulating T cell signaling pathways downstream of Zap-70.** *A, left,* elevated PLCγ1 activation in *Sts-1*$^{-/-}$, *Sts-2*$^{-/-}$, and *Sts-1/2*$^{-/-}$ activated, cultured T cells. T cells were lysed after stimulation for 2 min. Whole-cell lysates were separated by SDS-PAGE and subjected to Western analysis with phospho-specific antibodies directed against PLCγ1 Tyr(P)-783. The same blot was reprobed with anti-PLCγ1 antibodies, as a loading control (see *lower blot*). A representative blot of three independent experiments is displayed. *Right,* quantification of levels of phospho-PLCγ1 Tyr(P)-783 in wild-type and mutant T cells was performed as described in the legend to Fig. 1. *B, left,* elevated MAPK activation wild-type and mutant T cells. Whole-cell lysates of stimulated T cells were subjected to Western analysis with anti-phospho-MAPK antibodies. The same blot was reprobed with anti-Erk1/2 antibodies, as a loading control (see *lower blot*). A representative blot of three independent experiments is displayed. (*right*) Quantification of levels of phospho-MAPK in wild-type and mutant T cells was performed as described above. *dKO*, double knock-out.

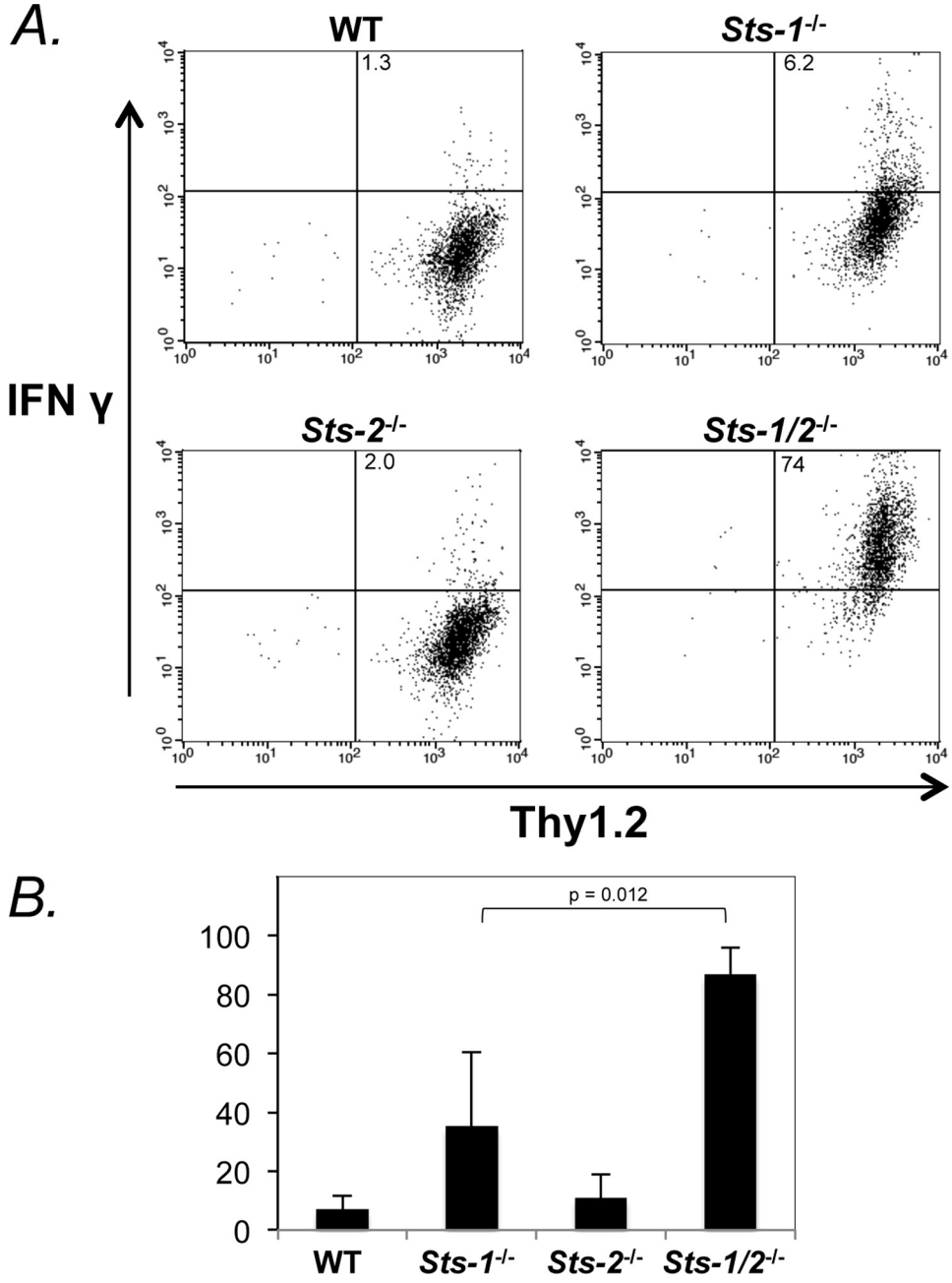

FIGURE 4. **Role for both Sts-2 and Sts-1 in regulating IFNγ expression.** *A,* T cells isolated from mutant mice were stimulated and 6 h later evaluated for levels of intracellular IFNγ by co-staining with antibodies to the T cell-specific marker Thy1.2 and to IFNγ. Cells lacking both Sts-1 and Sts-2 expressed higher levels of IFNγ relative to levels produced by wild-type, *Sts-1*$^{-/-}$, and *Sts-2*$^{-/-}$ cells. The percentage of T cells expressing IFNγ (double-positive) is indicated in the *upper right quadrant*. Representative FACS plots are illustrated. *B,* average percentage of T cells expressing IFNγ in three separate experiments is indicated.

cell and the context in which TCR stimulation occurs (24). T cells lacking the Sts proteins have been shown to secrete dramatically increased levels of several cytokines, including IFNγ relative to wild-type T cells (7). To determine the contribution of each Sts protein to the TCR-induced up-regulation of IFNγ expression, we evaluated levels of IFNγ induced in T cells derived from wild-type, *Sts-1*$^{-/-}$, *Sts-2*$^{-/-}$, and *Sts-1/2*$^{-/-}$ mice following TCR stimulation. As illustrated in Fig. 4, both Sts-1-deficient and Sts-2-deficient T cells expressed levels of IFNγ that were significantly less than the levels produced by *Sts-1/2*$^{-/-}$ T cells. The consistent production of greater IFNγ levels in *Sts-1*$^{-/-}$ T cells relative to levels in *Sts-2*$^{-/-}$ T cells paralleled the consistent increase in activation of different signaling molecules in *Sts-1*$^{-/-}$ cells relative to *Sts-2*$^{-/-}$ cells. As with the latter results, the levels of IFNγ production by the mutant T cells support the notion that Sts-1 and Sts-2 contribute distinct negative regulatory functions within T cell signaling pathways.

Phosphatase Activity of Sts-2—We have recently shown that the *in vitro* phosphatase activity of Sts-2_{PGM} toward pNPP is 5 orders of magnitude weaker that that of Sts-1_{PGM}, despite conservation of all catalytic residues (12). We argued that a possible explanation for this difference is the nature of the substrate rather than a lack of intrinsic phosphatase activity. To deter-

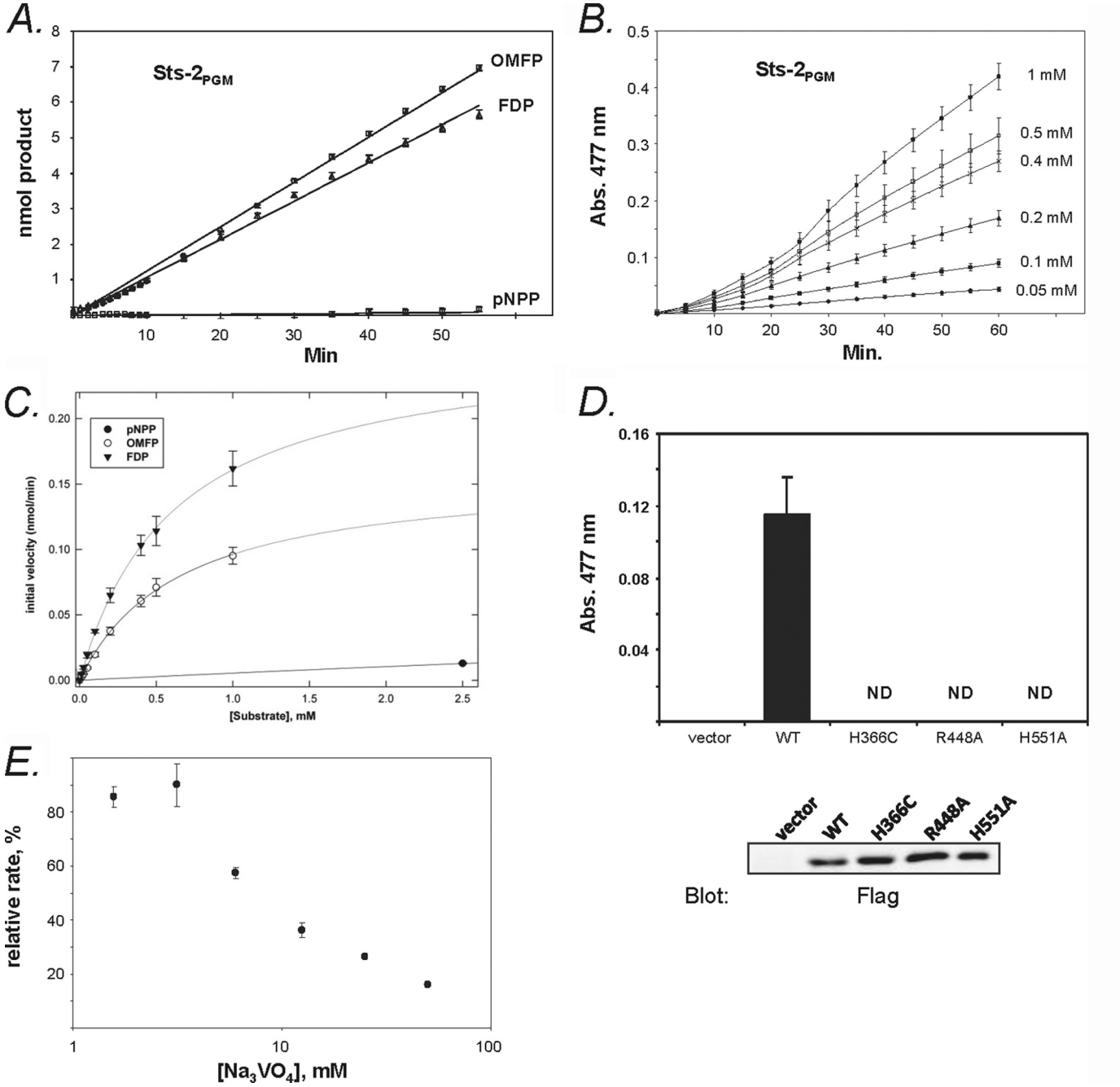

FIGURE 5. **PGM domain of Sts-2 has intrinsic phosphatase activity.** *A,* time course of phosphate hydrolysis by recombinant Sts-2_{PGM} (250 nM) using OMFP (0.5 mM), FDP (0.2 mM), and pNPP (0.5 mM) as substrates. *B,* time course of OMFP hydrolysis by recombinant Sts-2_{PGM} (150 nM) using various concentrations of OMFP (0.05–1 mM). *C,* substrate saturation curves for Sts-2_{PGM} against pNPP, OMFP, and FDP. *D,* OMFP hydrolysis activity of wild-type Sts-2_{PGM} or Sts-2_{PGM} active site mutants (H366C, R448A, and H551A). FLAG-tagged PGM domains were expressed in HEK293 cells, immunoprecipitated with M2 anti-FLAG antibody, and immobilized on protein A-Sepharose beads. The phosphatase assay was performed by adding 0.5 mM OMFP to the beads and incubating at 37 °C for 1 h. Assays were conducted in triplicate, and representative protein levels for each reaction were identified with FLAG antibodies. *E,* inhibition of Sts-2_{PGM} phosphatase activity by vanadate. Activity of recombinant Sts-2_{PGM} (150 nM) against OMFP (0.5 mM) was measured in the presence of increasing amounts of orthovanadate (1.56–50 mM). Rates were calculated from the slopes of the time course of the reaction and presented as ratios relative to the uninhibited (no vanadate) reaction.

mine whether other molecules might be hydrolyzed with greater efficiency by Sts-2_{PGM}, we evaluated phosphorylated fluorescein analogues as possible substrates. Phosphorylated fluorescein compounds have been developed as readily available tools to study the activity of protein-tyrosine phosphatases (25, 26). Fig. 5*A* illustrates that recombinant Sts-2_{PGM} dephosphorylates *O*-methylfluorescein phosphate (OMFP) and FDP, and it does so with significantly greater efficiency than it hydrolyzes pNPP. Notably, 20-fold lower Sts-2_{PGM} concentrations are needed to achieve measurable reaction velocities with OMFP and FDP than with pNPP, resulting in higher specific activities for the fluorescein analogues. For example, as estimated from assays in which the concentrations of pNPP and OMFP were 0.5 mM and FDP was 0.2 mM, the Sts-2_{PGM} specific

TABLE 1
Comparison of enzyme activities
Specific activities are shown in nmol/min/mg protein. Enzyme reactions were conducted in triplicate, as described under "Experimental Procedures." Concentration of pNPP and OMFP was 0.5 mM, and FDP was at 0.2 mM.

Enzyme	Substrate		
	pNPP	OMFP	FDP
Sts-2_{PGM}	1.6	72.3	58.1
Sts-1_{PGM}	10290	15700	8630
PTP1B	26490	21060	13320

TABLE 2
Activity constants of Sts-2_{PGM}

Enzyme	Substrate	K_m	k_{cat}	k_{cat}/K_m
		mM	s^{-1}	$M^{-1} s^{-1}$
Sts-2_{PGM}	pNPP[a]	2.0 ± 0.13	0.03	15
	OMFP	0.65 ± 0.05	0.18	271
	FDP	0.61 ± 0.03	0.29	472

[a] This is as determined previously (12).

activities were 72.3 nmol/min/mg protein (OMFP) and 58.1 nmol/min/mg (FDP) *versus* 1.6 nmol/min/mg (pNPP) (see Table 1). Thus, Sts-2_{PGM} exhibits 30–50-fold more activity toward the fluorescein-based compounds than toward pNPP.

Further analysis into the hydrolysis of OMFP by Sts-2_{PGM} demonstrated that the reaction follows Michaelis-Menten kinetics in which increases in substrate concentration result in faster initial reaction velocities (Fig. 5*B*). The phosphatase reaction was performed at multiple substrate concentrations (12.5 μM to 1 mM), and the initial velocity at each substrate concentration was plotted (Fig. 5*C*). As expected, the estimated specificity constants (k_{cat}/K_m) for the Sts-2_{PGM}-catalyzed hydrolysis of FDP and OMFP were found to be greater than Sts-2_{PGM} hydrolysis of pNPP (see Table 2). This is due both to significantly lower K_m values and to significantly greater k_{cat} values for the reactions involving the fluorescein compounds. The finding that OMFP is a better substrate than pNPP is not unprecedented. Previous work on Cdc25B, a dual specificity phosphatase, also demonstrated that OMFP is a better substrate than pNPP with an 810-fold greater specificity constant (27).

Like all PGM family members, Sts-2_{PGM} is characterized by a unique α/β core structure that consists of an inner parallel β sheet surrounded by a series of α helices and a catalytic core formed in part by several conserved active site residues, including His-366, Arg-448, and His-551, that cluster together (12). His-366 is the proposed nucleophile in the phosphatase reaction and is likely transiently phosphorylated during the catalytic reaction (28). To confirm that Sts-2_{PGM}-mediated dephosphorylation of OMFP represented a *bona fide* 2H phosphatase reaction, His-366, Arg-448, and His-551 were individually mutated to non-functional, and the activities of the resulting single point mutants were assessed. As shown in Fig. 5*D*, each mutation inactivated Sts-2_{PGM}, consistent with the hypothesis that the phosphatase activity of Sts-2_{PGM} is likely an intrinsic property derived from evolutionarily conserved active site residues common to all members of the PGM/AcP family. This model is strengthened by the observation that orthovanadate, a commonly used phosphotyrosine phosphatase inhibitor, can inhibit the dephosphorylation of OMFP by Sts-2_{PGM} (Fig. 5*E*). X-ray crystallographic studies have indicated that vanadate binds to the active site of Sts-2_{PGM} and interacts noncovalently with the nucleophilic residue His-366 (28).

Differences between Sts-2 and Sts-1 Catalytic Efficiency—As alluded to above, our prior work has demonstrated that Sts-2_{PGM} phosphatase activity toward the substrate pNPP is close to 5 orders of magnitude less than that of Sts-1_{PGM}. Additionally, although Sts-1_{PGM} can readily dephosphorylate tyrosine-phosphorylated peptides and proteins *in vitro*, Sts-2_{PGM}-mediated hydrolysis of peptide and polypeptide substrates *in vitro* is difficult to detect (supplemental Fig. S2) (12). Thus, Sts-2_{PGM} is significantly less active relative to Sts-1_{PGM}. An important question is whether this is due to the weak intrinsic phosphatase activity of Sts-2_{PGM} or does the choice and nature of the substrate matter? To address this, we compared the abilities of Sts-2_{PGM} and Sts-1_{PGM} enzymes to hydrolyze FDP and OMFP. Relative phosphatase activities utilizing either bacterially expressed recombinant Sts_{PGM} domains (Fig. 6*A* and Table 1) or Sts_{PGM} domains expressed in eukaryotic cells (Fig. 6*B*) or endogenous Sts proteins obtained from T cells (Fig. 6*C*) were evaluated. In each case, Sts-2 was found to be significantly less active than Sts-1. For example, the specific activity (0.5 mM substrate) of recombinant Sts-2_{PGM} toward OMFP was 72.3 nmol/min/mg, whereas the activity of recombinant Sts-1_{PGM} was 15,705 nmol/min/mg (Table 1). This represents an ~200-fold difference between the two phosphatases in hydrolytic activity toward the fluorescein-based compounds. In stark contrast, Sts-2_{PGM} exhibited a 6000-fold difference in activity toward pNPP relative to Sts-1_{PGM}. Interestingly, Sts-1_{PGM} displayed a similar activity as protein-tyrosine phosphatase 1B (PTP1B).

We have hypothesized that the difference in hydrolytic activity between the two Sts PGM enzymes stems from differences in noncatalytic, nonconserved active residues (12). Such residues could affect both the orientation and/or movements of critical catalytic residues or influence the manner in which phosphorylated substrates are positioned within the active site. Recent structural and mutagenesis analysis suggests that the nonconserved Sts-2 residues Glu-481, Ser-552, and Ser-582 are among the amino acids that contribute to the dramatic differences in Sts-2 phosphatase activity between Sts1- and Sts-2 (12). Specifically, these three amino acids, unlike their counterparts in Sts-1 (Val-495, Ala-566, and Tyr-596) are within hydrogen bond distances of critical catalytic residues and so might restrict their movement during catalysis (Fig. 7*A*). For example, Glu-481 makes a stabilizing hydrogen bond interaction with Arg-448, a basic residue that is thought to be involved in correctly positioning the negatively charged phosphate moiety of the substrate (27). Additionally, Glu-481 results in a negative charge situated close to acidic Glu-476, which is a conserved residue whose counterpart in other PGM family members has been proposed to act as a general acid/base during the catalytic reaction. As a result, Glu-476 is forced into a different conformation within the Sts-2_{PGM} active site than its counterpart in the active site of Sts-1_{PGM}. To evaluate whether Sts-2 residues Glu-481, Ser-552, and Ser-582 are among the residues responsible for the weaker phosphatase activity of Sts-2, we generated the VAY (E481V, S552A, S582Y) triple mutant of Sts-2_{PGM} in

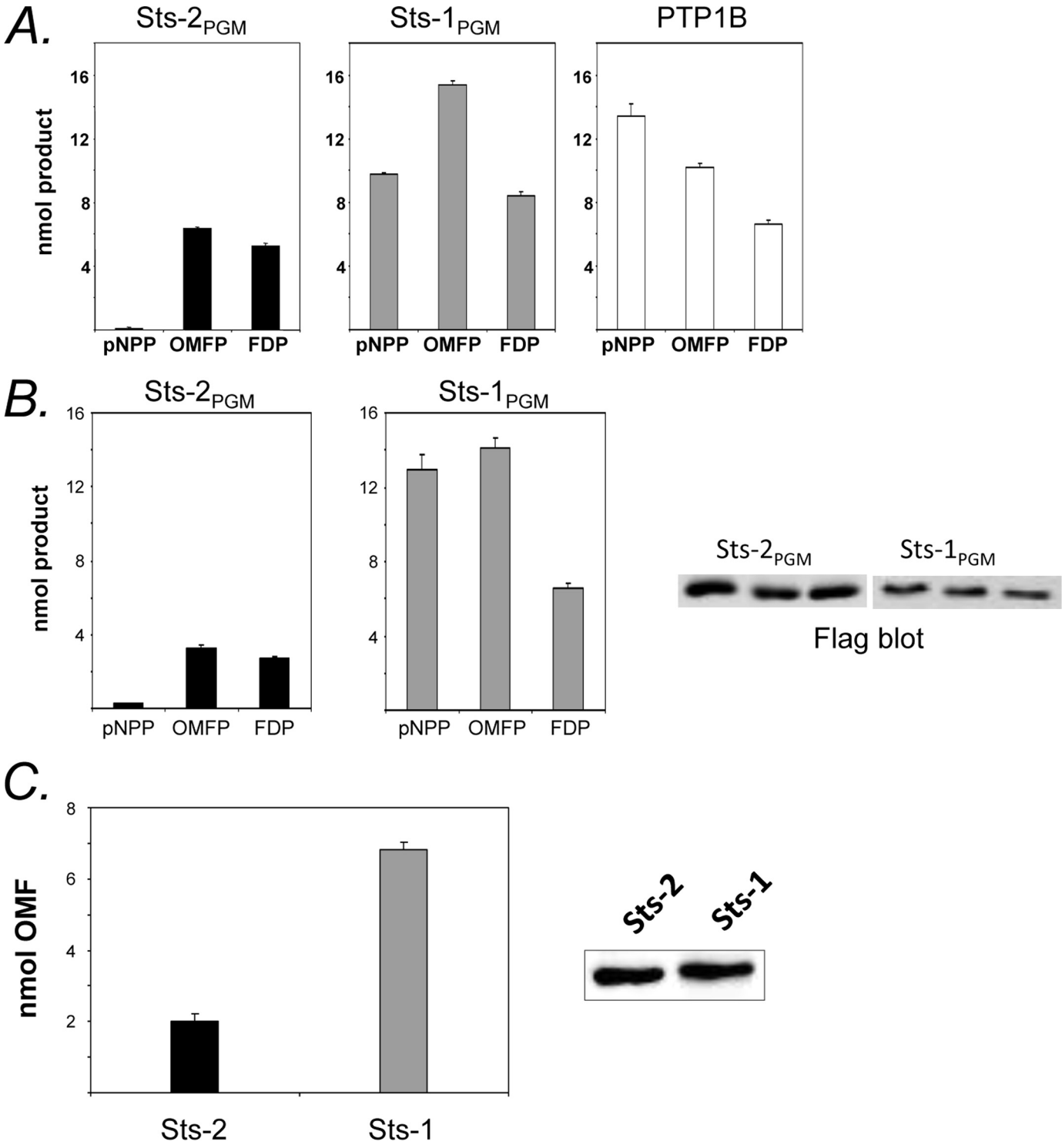

FIGURE 6. ***In vitro*, Sts-2_{PGM} is a weak phosphatase relative to Sts-1_{PGM}.** *A*, recombinant Sts-2_{PGM} (250 nM), Sts-1_{PGM} (25 nM), and PTP1B (25 nM) were assayed against 0.5 mM pNPP, 0.5 mM OMFP, and 0.2 mM FDP. The Sts-2_{PGM} reaction was allowed to proceed for 50 min, and the Sts-1_{PGM} and PTP1B reactions were stopped after 5 min. *B*, FLAG-tagged wild-type Sts-2_{PGM} and Sts-1_{PGM} were expressed in HEK293 cells and immunoprecipitated using anti-FLAG antibody, and phosphatase activity was assessed with 0.5 mM pNPP, 0.5 mM OMFP, and 0.2 mM FDP. The reactions were allowed to proceed as in *A*. Assays were conducted in triplicate, and representative protein levels for each reaction are illustrated (*right*). *C*, endogenously expressed Sts-2 and Sts-1 were immunoprecipitated from mouse primary T cells using rabbit polyclonal antibodies specific for each Sts protein, immobilized on protein A-Sepharose beads, and assayed for phosphatase activity with 0.5 mM OMFP at 37 °C for 75 min (Sts-2) or 10 min (Sts-1). Values obtained from precipitation reactions in which no specific antibodies were added served as blank values and were subtracted from values obtained in the experimental samples. Assays were conducted in triplicate, and representative protein levels for each reaction were identified with anti-Sts-1 and anti-Sts-2 antibodies (*right*).

which each amino acid was altered to its counterpart in Sts-1. With either pNPP (wild type: $K_m = 2$ mM, $k_{cat} = 0.03\ s^{-1}$; VAY: $K_m = 0.59$ mM, $k_{cat} = 1.3\ s^{-1}$) or OMFP (Fig. 7*B*), the VAY mutant was significantly more active than wild-type Sts-2_{PGM}. Thus, mutating nonconserved residues of Sts-2_{PGM} to their counterparts in Sts-1_{PGM} substantially increases the activity of

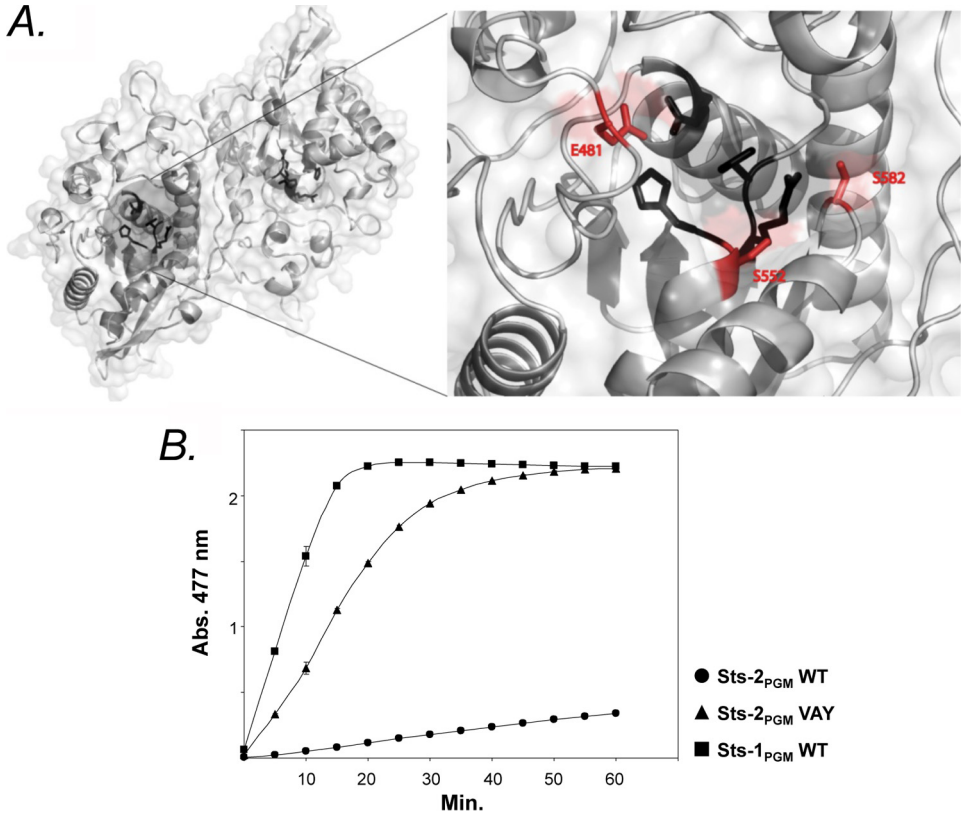

FIGURE 7. **Nonconserved residues adjacent to the active site contribute to differences between Sts-2_{PGM} and Sts-1_{PGM} catalytic activity.** *A,* ribbon and surface representation of the Sts-2_{PGM} dimer with a zoom in on the active site. The four invariant residues (two His and two Arg) of the catalytic core are shown in *black*. The nonconserved residues between Sts-2_{PGM} and Sts-1_{PGM} (Glu-481, Ser-552, and Ser-582) are labeled and shown in *red*. These residues are conserved in Sts-1 as Val-495, Ala-566, and Tyr-596, respectively. Figure was prepared with PyMol. *B,* Sts-2_{PGM} VAY triple mutant was generated by site-directed mutagenesis, altering Sts-2_{PGM} residues (Glu-481, Ser-552, and Ser-582) for the corresponding residues found in Sts-1_{PGM} (Val, Ala, and Tyr, respectively). Phosphate hydrolysis activities of recombinant Sts-2_{PGM} VAY, wild-type Sts-2_{PGM}, and wild-type Sts-1_{PGM} toward OMFP were compared. The reactions contained 0.5 mM OMFP and 100 nM Sts-2_{PGM}, 100 nM Sts-2_{PGM} VAY, or 10 nM Sts-1_{PGM} and were performed in triplicate.

Sts-2_{PGM} toward two model substrates. This suggests that Glu-481, Ser-552, and Ser-582 might be key specificity determinants that regulate the interaction of Sts-2_{PGM} with its substrate(s).

DISCUSSION

Our results firmly establish the distinct role of Sts-2 as a negative regulator of TCR signaling, acting through a mechanism that involves dephosphorylation of key signaling components such as Zap-70. Because of the extraordinarily poor catalytic efficiency of Sts-2_{PGM} toward all previously tested artificial substrates, it has long been unclear whether Sts-2 could act as an intracellular phosphatase. However, that Sts-2 is a catalytically active phosphatase is placed on firm ground by the clear display of Sts-2_{PGM} enzyme activity toward OMFP and FDP. At the present time, it is not clear why Sts-2_{PGM} prefers these two latter molecules over pNPP. It has been noted that OMF has a substantially lower pK_a than *p*-nitrophenol, making OMFP generally a more reactive substrate (27). It is also possible that the relatively larger size and orthogonal planes of the fluorescein-based compounds ensure a more energetically favorable orientation of the phosphate moiety within the Sts-2_{PGM} active site than occurs with the smaller phenyl ring of pNPP. If so, it might suggest that substrate conformation(s) is more critical for Sts-2_{PGM} than for the more promiscuous Sts-1_{PGM}. Whether this indicates a more limited subset of *in vivo* substrates for Sts-2 than Sts-1 is currently unclear. Nonetheless, by highlighting the phosphatase activity associated with the Sts-2 C-terminal PGM domain, our results suggest a mechanistic basis for how the Sts homologues cooperate in a similar fashion to help set the threshold for TCR-induced T cell activation. Given the shared domain structure of Sts-1 and Sts-2, a mechanism of action for both proteins is postulated to involve PGM domain phosphatase effector activity acting in concert with the unique protein binding properties of their respective UBA and SH3 domains. Therefore, we propose that a catalytically active PGM domain phosphatase domain is necessary for the ability of Sts-2 to act as an intracellular phosphatase that regulates both Zap-70 tyrosine phosphorylation and the level of phosphorylation within the population of TCR-induced tyrosine-phosphorylated, ubiquitinated proteins. Whether Sts-2 phosphatase activity targets Zap-70 directly or indirectly is currently unclear, given our inability to observe Sts-2_{PGM}-mediated dephosphorylation of Zap-70 *in vitro* (supplemental Fig. S2).

Although our previous reports identified the critical T cell tyrosine kinase Zap-70 as a potential downstream target of Sts activity (7, 11), the individual contributions of each Sts protein to the regulation of Zap-70 had not been established. Our current data indicate that Sts-2 has a distinct regulatory role, a finding that is underscored by the observation that the combined loss of both Sts proteins (*Sts-1/2*$^{-/-}$) has a greater effect on the hyper-activation of signaling pathways than the loss of

Sts-1 alone. Interestingly, the effects of Sts-2 deficiency are not always readily apparent in cells that express Sts-1, suggesting that Sts-1 can to a limited extent compensate for the loss of Sts-2. Thus, the present data illustrate that Sts-1 and Sts-2 each target Zap-70 in separate but overlapping fashions.

Judging by the extent of Zap-70 hyper-phosphorylation in *Sts-1*$^{-/-}$ and *Sts-2*$^{-/-}$ T cells, the *in vivo* phosphatase activity of Sts-2 is less than Sts-1. Additionally, the population of proteins that are dually modified by tyrosine phosphorylation and ubiquitination following TCR stimulation that have been identified as likely Sts targets also appear to be targeted by Sts-1 and Sts-2 in separate but overlapping manners, with Sts-2 also appearing to be less efficient *in vivo*. It is noteworthy that *in vitro* the two PGM domains exhibit markedly different enzymatic activity, with weak Sts-2_{PGM} phosphatase activity standing in stark contrast to the potent activity of Sts-1_{PGM}. The direct correlation between the *in vitro* catalytic efficiency of each PGM phosphatase domain and the phosphorylation levels observed in mutant T cells implies a clear functional relevance for the disparate enzymatic activities as measured *in vitro* associated with each Sts protein. However, it is important to keep in mind that the manner in which the Sts-1 and Sts-2 interact with their intracellular substrate(s) is not fully established. Therefore, it is possible that the N-terminal UBA and SH3 protein interaction domains of each Sts protein contribute to their unique *in vivo* functional properties.

To date, evidence for the role of Sts-2 as an intracellular phosphatase with negative regulatory functions has been limited. Initially, the apparent absence of Sts-2_{PGM} activity raised the possibility that Sts-2 might function not as a phosphatase but rather as a naturally occurring, T cell-specific dominant inhibitor of Sts-1 phosphatase functions (17). Other proposed cellular functions of Sts-2 are thought to be mediated by domains other than the PGM domain. Instead, these functions appear to require the nonenzymatic UBA and SH3 domains. For example, a role for inhibiting tyrosine kinase receptor endocytosis by preventing endocytic adaptor proteins access to ubiquitinated receptor complexes is thought to be mediated both by the UBA domain interacting with mono-ubiquitinated receptor and the SH3 domain interacting with the E3 ubiquitin ligase/adaptor protein, Cbl (29). In addition, a role promoting caspase-independent apoptosis via interaction with apoptosis-inducing factor was demonstrated to involve primarily the UBA and SH3 domains together (30).

Aside from this study, there is additional compelling evidence in support of a role for Sts-2 as an intracellular phosphatase. This evidence includes the remarkably close structural similarity between Sts-2_{PGM} and the strongly active phosphatase Sts-1_{PGM} (11, 12), as well as the evolutionary conservation of all critical catalytic residues in all Sts-2 homologues. It is worth noting that several members of the class I cysteine-based protein-tyrosine phosphatase family of phosphatases are functionally similar to Sts-2 in that they have little or no measurable *in vitro* phosphatase activity on peptide substrates yet are thought to act *in vivo* as tyrosine phosphatases (31–33). Given the interesting difference between the *in vivo* and *in vitro* observations, we speculate that Sts-2_{PGM} enzymatic activity is regulated *in vivo* by a mechanism that is currently unclear. Unlike protein-tyrosine phosphatases, which have a prominent structural element known as the WPD loop whose movements adjacent to the active site affect catalytic activity (34), to date the PGM domain of Sts-2 appears to have no intrinsic structural component that regulates its enzymatic activity. It is tempting to speculate that the *in vivo* mechanism of regulation of Sts-2_{PGM} phosphatase activity is a specific property of T cells, as these are the cells within which Sts-2 is almost exclusively expressed. Addressing the unique requirement for Sts-2 expression in T cells and how Sts-2_{PGM} phosphatase activity is regulated in the context of its ability to negatively regulate TCR signaling is a focus of ongoing research.

Acknowledgments—We thank Laurie Levine for assistance with animal care. We also thank Jorge Benach for unfailing support and N. Reich and M. Hayman for helpful discussions.

REFERENCES

1. Chaplin, D. D. (2010) *J. Allergy Clin. Immunol.* **125,** S3–S23
2. Huston, D. P. (1997) *JAMA* **278,** 1804–1814
3. Huang, Y., and Wange, R. L. (2004) *J. Biol. Chem.* **279,** 28827–28830
4. Acuto, O., Di Bartolo, V., and Michel, F. (2008) *Nat. Rev. Immunol.* **8,** 699–712
5. Tsygankov, A. Y. (2009) *Cell. Mol. Life Sci.* **66,** 2949–2952
6. Carpino, N., Chen, Y., Nassar, N., and Oh, H. W. (2009) *Mol. Immunol.* **46,** 3224–3231
7. Carpino, N., Turner, S., Mekala, D., Takahashi, Y, Zang, H., Geiger, T. L., Doherty, P., and Ihle, J. N. (2004) *Immunity* **20,** 37–46
8. Hoeller, D., Crosetto, N., Blagoev, B., Raiborg, C., Tikkanen, R., Wagner, S., Kowanetz, K., Breitling, R., Mann, M., Stenmark, H., and Dikic, I. (2006) *Nat. Cell Biol.* **8,** 163–169
9. Jedrzejas, M. J. (2000) *Prog. Biophys. Mol. Biol.* **73,** 263–287
10. Rigden, D. J. (2008) *Biochem. J.* **409,** 333–348
11. Mikhailik, A., Ford, B., Keller, J., Chen, Y., Nassar, N., and Carpino, N. (2007) *Mol. Cell* **27,** 486–497
12. Chen, Y., Jakoncic, J., Carpino, N., and Nassar, N. (2009) *Biochemistry* **48,** 1681–1690
13. Chen, X., Ren, L., Kim, S., Carpino, N., Daniel, J. L., Kunapuli, S. P., Tsygankov, A. Y., and Pei, D. (2010) *J. Biol. Chem.* **285,** 31268–31276
14. Raguz, J., Wagner, S., Dikic, I., and Hoeller, D. (2007) *FEBS. Lett.* **581,** 4767–4772
15. Agrawal, R., Carpino, N., and Tsygankov, A. (2008) *J. Cell. Biochem.* **104,** 953–964
16. Feshchenko, E. A., Smirnova, E. V., Swaminathan, G., Teckchandani, A. M., Agrawal, R., Band, H., Zhang, X., Annan, R. S., Carr, S. A., and Tsygankov, A. Y. (2004) *Oncogene* **23,** 4690–4706
17. Tsygankov, A. Y. (2008) *IUBMB Life* **60,** 224–231
18. Carpino, N., Kobayashi, R., Zang, H., Takahashi, Y., Jou, ST., Feng, J., Nakajima, H., and Ihle, J. N. (2002) *Mol. Cell. Biol.* **22,** 7491–7500
19. Kleinman, H., Ford, B., Keller, J., Carpino, N., and Nassar, N. (2006) *Acta Crystallogr. Section F Struct. Biol. Cryst. Commun.* **62,** 218–220
20. Au-Yeung, B. B., Deindl, S., Hsu, L. Y., Palacios, E. H., Levin, S. E., Kuriyan, J., and Weiss, A. (2009) *Immunol. Rev.* **228,** 41–57
21. Wang, H., Kadlecek, T. A., Au-Yeung, B. B., Sjolin Goodfellow, H. E., Hsu, L. Y., Freedman, T. S., and Weiss, A. (2010) *Cold Spring Harbor Perspect. Biol.* **2,** 1–17
22. Singer, W. D., Brown, H. A., and Sternweis, P. C. (1997) *Annu. Rev. Biochem.* **66,** 475–509
23. Wang, Z., Glück, S., Zhang, L., and Moran, M. F. (1998) *Mol. Cell. Biol.* **18,** 590–597
24. Siegel, J. N., Egerton, M., Phillips, A. F., and Samelson, L. E. (1991) *Semin. Immunol.* **3,** 325–334
25. Huang, Z, Wang, Q., Ly, H. D., Gorvindarajan, A., Scheigetz, J., Zamboni,

R., Desmarais, S., and Ramachandran, C. (1999) *J. Biomol. Screen.* **6,** 327–334
26. Wang, Q., Scheigetz, J., Gilbert, M., Snider, J., and Ramachandran, C. (1999) *Biochim. Biophys. Acta* **1431,** 14–23
27. Gottlin, E. B., Xu, X., Epstein, D. M., Burke, S. P., Eckstein, J. W., Ballou, D. P., and Dixon, J. E. (1996) *J. Biol. Chem.* **271,** 27445–27449
28. Chen, Y., Jakoncic, J., Parker, K. A., Carpino, N., and Nassar, N. (2009) *Biochemistry* **48,** 8129–8135
29. Kowanetz, K., Crosetto, N., Haglund, K., Schmidt, M. H., Heldin, C. H., and Dikic, I. (2004) *J. Biol. Chem.* **279,** 32786–32795
30. Collingwood, T. S., Smirnova, E. V., Bogush, M., Carpino, N., Annan, R. S., and Tsygankov, A. Y. (2007) *J. Biol. Chem.* **282,** 30920–30928
31. Barr, A. J., Ugochukwu, E., Lee, W. H., King, O. N., Filippakopoulos, P., Alfano, I., Savitsky, P., Burgess-Brown, N. A., Müller, S., and Knapp, S. (2009) *Cell* **136,** 352–363
32. Cardone, L., Carlucci, A., Affaitati, A., Livigni, A., DeCristofaro, T., Garbi, C., Varrone, S., Ullrich, A., Gottesman, M. E., Avvedimento, E. V., and Feliciello, A. (2004) *Mol. Cell. Biol.* **24,** 4613–4626
33. Wadham, C., Gamble, J. R., Vadas, M. A., and Khew-Goodall, Y. (2003) *Mol. Biol. Cell.* **14,** 2520–2529
34. Barford, D., Das, A. K., and Egloff, M. P. (1998) *Annu. Rev. Biophys. Biomol. Struct.* **27,** 133–164